Sensors and Materials, Vol. 32, No. 5 (2020) 1843–1850
MYU Tokyo

S & M 2222

Fabrication of Non-enzymatic Ni–Au Alloy Nanowire Glucose Sensor

Yi-Shu Hsieh,[1] Po-Wen Wang,[1] Chien-Yu Li,[1] Shang-Ju Hsieh,[1]
Ching-Yu Wang,[1] Dei-Wei Chou,[2] Na-Fu Wang,[3] and Mau-Phon Houng[1*]

[1]Department of Electrical Engineering, Institute of Microelectronics,
National Cheng Kung University, No. 1, University Rd, Tainan 701, Taiwan
[2]Department of Military Meteorology, Air Force Institute of Technology, Kaohsiung 820, Taiwan
[3]Department of Electronic Engineering, Center for Environmental Toxin and Emerging-Contaminant Research,
Super Micro Mass Research & Technology Center, Cheng Shiu University,
No. 840, Chengcing Rd, Niaosong Dist., Kaohsiung City 83347, Taiwan

(Received April 24, 2019; accepted April 22, 2020)

Keywords: non-enzymatic, glucose sensor, Ni–Au alloy nanowire, anodic aluminum oxide (AAO)

We fabricated a non-enzymatic Ni–Au alloy nanowire electrochemical glucose sensor on a p-silicon-based anodic aluminum oxide (AAO) template. The advantages of the Ni–Au glucose sensor are its high sensitivity and stability, and fast reaction. In contrast to a traditional enzymatic glucose sensor, the non-enzymatic glucose sensor is reusable, enabling its long-term use by patients with diabetes. Although the reduction voltages of Ni and Au are considerably different, the Ni–Au alloy nanowires used in the sensor were fabricated successfully via the adjustment of the electrodeposition parameters. The Ni–Au alloy nanowires exhibited a high crystallinity and a uniform arrangement with an average height of 750 nm. The Ni–Au alloy glucose sensor exhibited a linear range of 0–3 mM, a sensitivity of 1893 μA/mMcm^2, and a detection limit of 1 μM. Superior selectivity and stability over at least 30 days were also observed. The characteristics show that Ni–Au alloy nanowires have excellent glucose-sensing performance compared with single noble metal nanowires. The silicon-based AAO template also serves as a strong mechanical support of the Ni–Au nanowires used for sensing. To our knowledge, our fabricated sensor is the first non-enzymatic glucose sensor to use Ni–Au alloy nanowires.

1. Introduction

An increasing number of people suffer from diabetes. Therefore, rapid and precise glucose sensors are becoming increasingly important. Commercial glucose sensors including spectrophotometric,[1–3] glucose, and electrochemical glucose sensors have been widely studied. An electrochemical glucose sensor exhibits the advantages of high sensitivity and stability, and a fast reaction. Electrochemical glucose sensors can be divided into enzymatic[4,5] and non-enzymatic glucose sensors.[6,7] Although enzymatic glucose sensors have a high sensitivity and a large measurement range, they are easily affected by pH, temperature, and humidity.[8,9] The

*Corresponding author: e-mail: mphoung@mail.ncku.edu.tw
https://doi.org/10.18494/SAM.2020.2479

ISSN 0914-4935

most serious problem is that their lifetime is too short for long-term use by diabetes patients. We have therefore focused on the fabrication of a non-enzymatic glucose sensor.

Owing to their advantages, many remarkable non-enzymatic glucose sensors with different structures and materials have been fabricated.[8–20] Among these sensors, those using nanostructures have the highest redox ability. Noble metal electrodes including Au[10] and Pt have also been used in glucose sensing. However, they have a low sensitivity and a high cost. Multilayer[9,11,12] and alloy structures[13–15] have been used to solve the problems of noble metal electrodes because of their synergistic effect. Some studies[9] have indicated that multilayer and alloy electrodes have better sensing characteristics because of their superior redox ability to a single-material electrode. Furthermore, the alloy structure can decrease the use of noble metals and reduce the total cost.

In this study, a Ni–Au alloy nanowire was successfully fabricated using laboratory-made anodic aluminum oxide (AAO) grown on a p-type heavily doped silicon substrate by three-electrode pulse electrodeposition. Then, the oxidation peak and the sensitivity of the sensing electrode were investigated in 0.1 M NaOH by cyclic voltammetry (CV) and observing the amperometric response.

2. Materials and Methods

2.1 Reagents and instruments

Acetone, methanol, oxalic acid, and dimethyl sulfoxide (DMSO) were obtained from JT Baker. Phosphate, glucose, amino acid (AA), and urea were purchased from Sigma-Aldrich. Boric acid and sodium hydroxide were purchased from Merck. Nickel chloride hexahydrate and tetrachloroauric acid tetrahydrate were obtained from Alfa Aesar. Uric acid (UA) was purchased from Acros Organics.

2.2 Deposition of aluminum and fabrication of AAO template

A p-type heavily doped silicon substrate was cleaned with hydrofluoric acid, acetone, methanol, and deionized water. First, the p-type heavily doped silicon substrate was soaked in hydrofluoric acid for 1 min. Then, it was washed and dried with deionized water and an air gun, respectively. Next, it was cleaned again for 5 min each with acetone, methanol, and deionized water in an ultrasonic machine. Finally, it was dried again with an air gun.

Figure 1 shows the fabrication flow diagram of the AAO template. After cleaning the substrate, an aluminum film was deposited on the p-type heavily doped silicon substrate via a thermal evaporator or by sputter deposition. After that, the substrate was annealed in a 400 ℃ furnace for 3 h. It was then soaked in oxalic acid for about 30 min to induce anodization. Then, it was immersed in phosphate for 35 min at 30 ℃ for pore etching. As shown in the scanning electron microscopy (SEM) image in Fig. 2(a), the diameter of each hole was about 79.4 nm. Figure 2(b) shows that the thickness of the aluminum film was about 1.25 μm. The appearance of the film made from AAO in Fig. 2 was not as good as that of the film made from pure

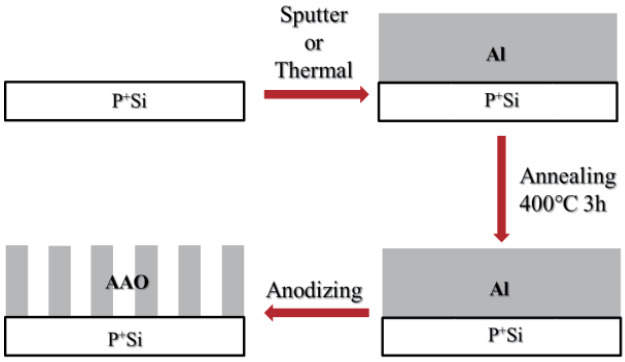

Fig. 1. (Color online) Fabrication flow diagram of AAO template.

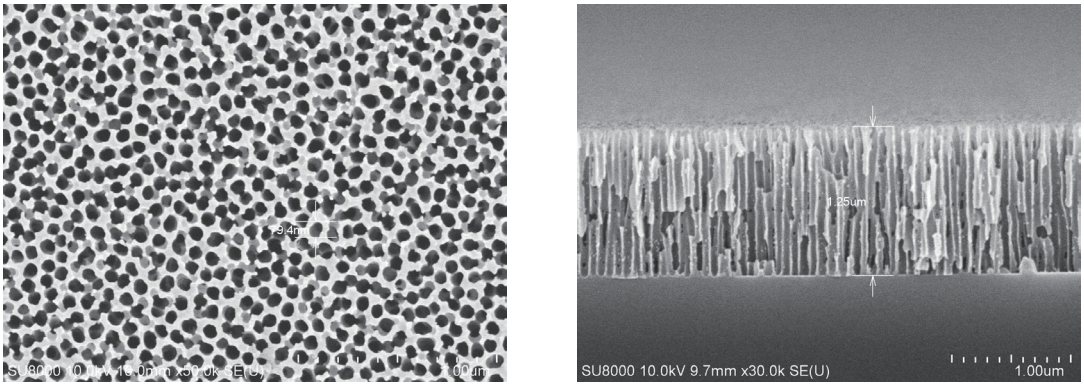

(a) (b)

Fig. 2. SEM images of laboratory-made AAO template: (a) top view and (b) cross section.

aluminum because different fabrication methods were used for the aluminum film AAO and the pure aluminum AAO. However, the hardness and fabrication time of the aluminum film AAO were much greater and shorter than those of the pure aluminum AAO, respectively.

2.3 Fabrication of Ni–Au alloy nanowires

Ni–Au alloy nanowires were deposited in a three-electrode deposition system. The electrolyte for Ni–Au electrodeposition was composed of 2.94 mM $HAuCl_4 \cdot 4H_2O$, 2.3 M $NiCl_2 \cdot 6H_2O$, 0.604 M H_3BO_3, and 3.75 M DMSO. A saturated calomel electrode was used as a reference electrode, while Pt was used as a counter electrode. Figure 3 shows the fabrication flow diagram of Ni–Au alloy nanowires. Before the deposition, the AAO samples were immersed in DMSO solution for at least 30 min to ensure surface polarity. The Ni–Au alloy nanowires were formed by alternate pulse deposition at −1.6 V for 1300 s with a duty cycle of 10% [T_{on} = 1 (s), T_{off} = 9 (s)]. After deposition, the samples were soaked in 2 M NaOH in 30 °C for 1 h to remove AAO. As shown in Fig. 4(a), holes were completely filled with Ni–Au alloy nanowires. Figure 4(b) shows that the Ni–Au alloy nanowires had a uniform arrangement with an average height of 750 nm.

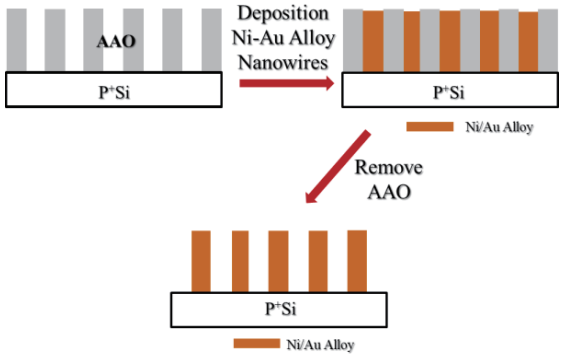

Fig. 3. (Color online) Fabrication flow diagram of Ni–Au alloy nanowires.

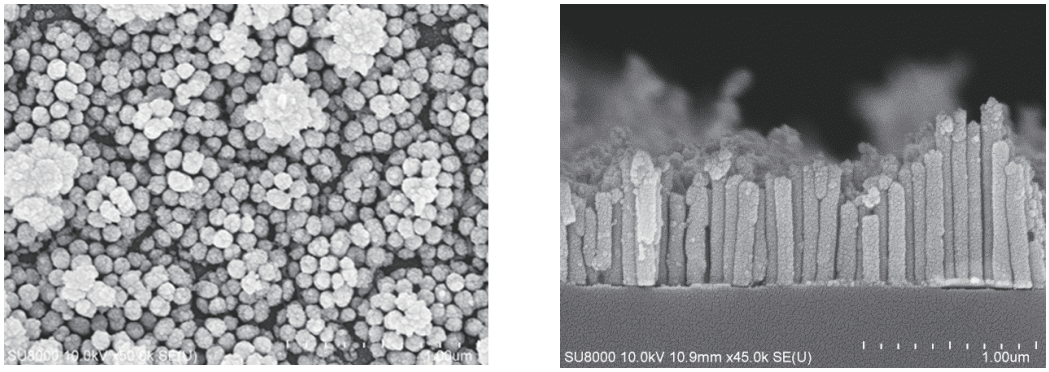

(a) (b)

Fig. 4. SEM images of Ni–Au nanowires: (a) top view and (b) cross section.

Table 1
Element ratio of Ni and Au in Ni–Au alloy nanowires.

Element	Atomic number	Element ratio (%)
Ni	28	48.74
Au	79	51.26

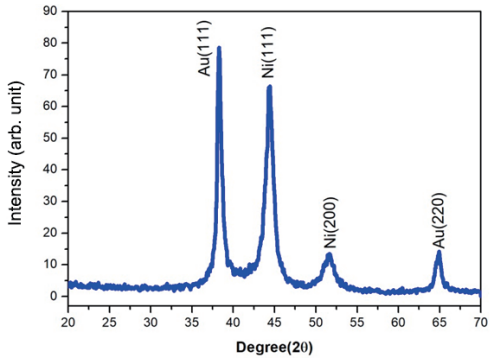

Fig. 5. (Color online) XRD spectrum of Ni–Au alloy nanowires.

Energy-dispersive spectrometry (EDS) was used to further analyze the element composition of the nanowires. As shown in Table 1, the nanowires consisted of about 50% Au and 50% Ni.

Figure 5 shows the XRD spectrum of the Ni–Au alloy nanowires. The two main peaks correspond to Au (111) and Ni (111) (JCPDS 04-0784 and 04-0850, respectively), proving that the nanowires mainly comprised Au and Ni.

3. Results and Discussion

3.1 Cyclic voltammograms and amperometric response

A 0.1 M NaOH solution was used to measure glucose owing to its strong oxidation characteristic. During the oxidation of the Ni–Au alloy nanowires in the electrode, CV was performed to accurately obtain the oxidation voltage. The reactions between the Ni–Au alloy nanowires, NaOH, and glucose can be expressed by Eqs. (1)–(5).[8–10] When Ni and Au react with a hydroxyl ion, they become NiO(OH) and AuOH, respectively, and release an electron. Glucose plays an important role in this reaction because it can convert NiO(OH) and AuOH back to Ni and Au. Through this loop, electrons continue to be released. Therefore, the current becomes larger than that in the absence of glucose.

$$Ni + 2OH^- \rightarrow Ni(OH)_2 \quad (1)$$

$$Ni\,(OH)_2 + OH^- \rightarrow NiO(OH) + H_2O + e^- \quad (2)$$

$$NiO(OH) + \text{glucose} \rightarrow Ni(OH)_2 + \text{glucolactone} \quad (3)$$

$$Au + OH^- \rightarrow AuOH + e^- \quad (4)$$

$$AuOH + \text{glucose} \rightarrow Au + \text{glucolactone} \quad (5)$$

The cyclic voltammogram of the Ni–Au alloy nanowires in 0.1 M NaOH, which is used to obtain the oxidation and reduction voltage of Ni–Au alloy in Fig. 6(a), has two peaks. The upper curve in this figure shows the anodic peak, which is caused by the oxidation current, and the other curve shows the cathodic peak, which is caused by the reduction current. The redox reaction and CV can be expressed by Eqs. (2) and (4), respectively. The oxidation peak is at 0.4–0.7 V (vs SCE) and the reduction peak is at 0.15 V (vs SCE). The scan rate of CV was 0.01 V/s; a too high scan rate would not have clearly revealed the oxidation peak.

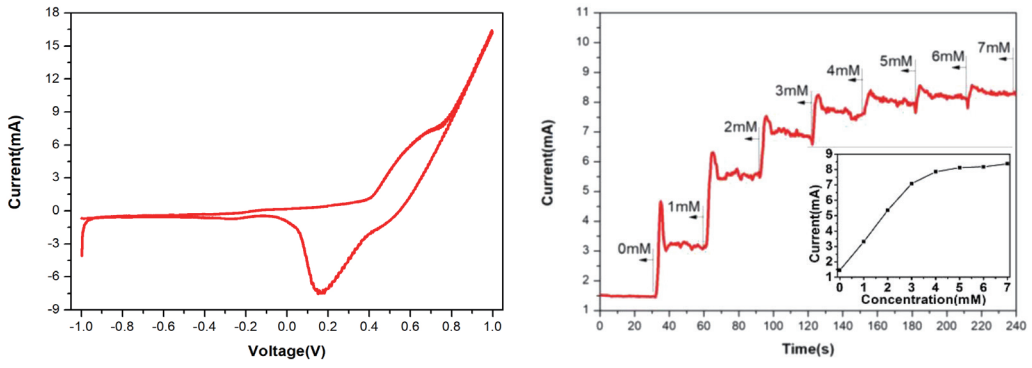

(a) (b)

Fig. 6. (Color online) (a) Cyclic voltammogram from −1 to 1 V of Ni–Au alloy nanowire electrode in 0.1 M NaOH. (b) Amperometric response of Ni–Au alloy nanowire electrode to addition of 0.6 ml of 1 M glucose in 0.1 M NaOH at 0.6 V (vs SCE). Inset: current versus concentration.

Figure 6(b) shows the amperometric response at a constant voltage of 0.6 V (vs SCE) in 0.1 M NaOH. Glucose solution was added every 30 s. Stirring was carried out during the experiment to ensure that the glucose solution was detected evenly. Owing to the fast reaction, the current decreased rapidly as shown in Fig. 6(b). To accurately record the current, the peak current before adding the glucose solution was used as an index to obtain the current versus concentration curve.

3.2 Sensitivity, linear range, selectivity, stability, and detection limit

The inset of Fig. 6(b) shows the current versus concentration curve. The relationship is linear in the range of 0–3 mM ($R^2 = 0.99858$). The sensitivity of the electrode can be calculated via

$$Sensitivity\ (\mu A/mMcm^2) = \frac{Current\,(\mu A)}{Concentration\,(mM) \times Area\,(cm^2)}. \tag{6}$$

Setting the area of the Ni–Au alloy nanowires in Eq. (6) to 1 cm^2, we obtained a sensitivity of 1893 μA/mMcm^2 for the electrode in the range of 0–3 mM.

The main application of this non-enzymatic glucose sensor is expected to be measuring blood sugar. However, other substances are present in blood. To ensure that other substances do not affect glucose sensing, we carried out a selectivity test. To simulate a similar environment to the human body, glucose, AA, urea, and UA were used to examine the selectivity of the sensor. Figure 7 shows the amperometric response of the Ni–Au alloy nanowires. It is clear that current is only generated with the addition of glucose. In other words, the proposed Ni–Au alloy nanowire electrode has excellent selectivity to glucose.

To obtain accurate measurement values, measurements were carried out to determine the detection limit. As shown in Fig. 8, the addition of 10, 50, and 100 μm glucose can be detected

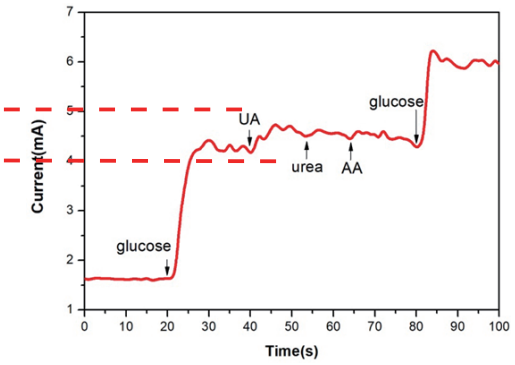

Fig. 7. (Color online) Amperometric response of Ni–Au alloy.

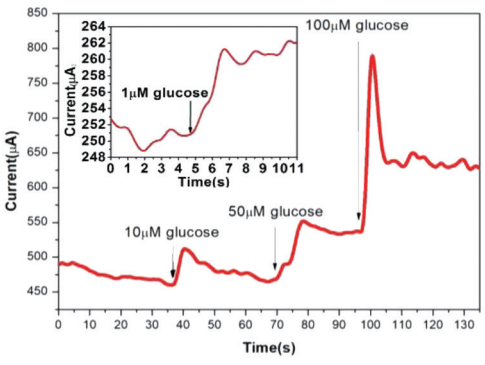

Fig. 8. (Color online) Amperometric response of Ni–Au alloy nanowire electrode to addition of small amounts of glucose solution. Inset: amperometric response of Ni–Au alloy nanowire electrode to addition of 1 μm of glucose solution, UA, urea, and AA.

Table 2
Comparison of proposed sensor with other non-enzymatic sensors.

Electrode material	Sensitivity ($\mu AmM^{-1}cm^{-2}$)	Linear range (mM)	Selectivity (Y/N)	Detection limit (μM)	Stability (days)	Reference
Ni nanowires	1043	0.0005–7	Y	0.1	65	8
Au nanowires	309	0–10	Y	50	60	9
CNT–Ni nanostructures	1300	0.5–10	Y	1	15	16
PtNi alloy nanoparticles	1795.1	0.002–0.42	Y	1	N/A	17
$Ni(OH)_2$–Au nanohybrid	371.2	0.005–2.2	Y	0.92	At least 21	18
Ni–Ag carbon nanotubes	2946	0–0.35	Y	0.062	At least 22	19
Au nanoparticles	160	0.5–8	Y	0.5	N/A	20
Au–Ni multilayer nanowires	3372	0.00025–2.2	Y	0.1	At least 21	10
Ni–Au alloy nanowires	1893	0.001–3	Y	1	At least 30	This work

by the Ni–Au alloy nanowire electrode. The inset shows that the addition of 1 μm glucose can also be detected. Therefore, the detection limit of the Ni–Au alloy nanowires is 1 μm. The stability of the electrode was also evaluated. After 30 days of measurement, the sensitivity was 95% of its original value, demonstrating the high stability of the Ni–Au alloy nanowire electrode.

Table 2 shows a comparison of the proposed sensor with other previously reported non-enzymatic sensors. Compared with the other sensors, the Ni–Au alloy nanowire electrode has a very high sensitivity, a wide linear range, a low detection limit, and a high stability.

4. Conclusion

Ni–Au alloy nanowires were fabricated using a laboratory-made AAO template fabricated on a p-type heavily doped silicon substrate. Despite the considerably different reduction voltages of Ni and Au, we successfully fabricated the Ni–Au alloy nanowires by adjusting the electrodeposition parameter. A sensor using Ni–Au alloy nanowires as the electrode exhibited excellent sensitivity, a wide linear range, a low detection limit, and a high stability, making it ideal for use as a non-enzymatic glucose sensor.

Acknowledgments

This work was supported by the Ministry of Science and Technology (MOST) of Taiwan under Contract Nos. MOST 107-2221-E-006-159 and MOST 108-2221-E-230-006.

References

1 L. Heinemann and G. Schmelzeisen-Redeker: Diabetologia **41** (1998) 848. https://link.springer.com/article/10.1007%2Fs001250050998?LI=true
2 J. B. Slate and P. C. Lord: U.S. Patent No. 5605152 (25 Feb. 1997). https://patents.google.com/patent/US5605152A/en
3 S. Mansouri and J. S. Schultz: Bio/Technology **2** (1984) 885. https://www.nature.com/articles/nbt1084-885
4 R. Wilson and A. P. F. Turner: Biosens. Bioelectron. **7** (1992) 165. https://www.sciencedirect.com/science/article/pii/095656639287013F

5 S. Changsheng, Y. Huafeng, S. Jiangfeng, H. Dongxue, A. Ivaska, and L. Niu: Anal. Chem. **81** (2009) 2378. https://pubs.acs.org/doi/abs/10.1021/ac802193c
6 L. Jing, J. Sisi, Z. Hongyan, J. Jinqiang, and L. XiaoyaLiu: Anal. Chim. Acta **709** (2012) 47. https://www.sciencedirect.com/science/article/pii/S0003267011013754
7 S. Park, H. Boo, and C. T. Dong: Anal. Chim. Acta **556** (2006) 46. https://www.sciencedirect.com/science/article/pii/S0003267005009864
8 L. Li-Min, Z. Li, Q. Feng-Li, L. Hai-Xia, Z. Xiao-Bing, W. Zai-Sheng, H. Shuang-Yan, W. Qiu-An, S. Guo-Li, and Y. Ru-Qin: Biosens. Bioelectron. **25** (2009) 218. https://www.sciencedirect.com/science/article/pii/S0925400509005784
9 Q. Lirong, H. Lizhong, Z. Jianwei, Z. Binglin, Y. Yingying, and Y. Yu: Sens. Actuators, B **240** (2017) 779. https://www.sciencedirect.com/science/article/pii/S0925400516314599
10 S. Cherevko and C.-H. Chung: Sens. Actuators, B **142** (2009) 216. https://www.sciencedirect.com/science/article/pii/S0925400509005784
11 C. Zhengbo, G. Junxia, Z. Tong, Z. Youwei, and C. Liang: Electrochim. Acta **109** (2013) 532. https://www.sciencedirect.com/science/article/pii/S0013468613015314
12 G. Zhi-Da, H. Yuyao, W, Yongmei, X. Jingwen, and S. Yan-Yan: Sci. Rep. **3** (2013) 3323. https://www.nature.com/articles/srep03323
13 C. Li, H. Wang, and Y. Yamauchi: Chem. Eur. J. **19** (2013) 2242. https://onlinelibrary.wiley.com/doi/full/10.1002/chem.201203378
14 C. Hui-Fang, Y. Jian-Shan, L. Xiao, Z. Wei-De, and S. Fwu-Shan: Nanotechnol. **17** (2006) 2334. https://iopscience.iop.org/article/10.1088/0957-4484/17/9/043/meta
15 N. Hui-Bog, L. Kyung-Sun, C. Pranjal, W. Mi-Sook, and S. Yoon-Bo.: Electrochim. Acta **61** (2012) 36. https://www.sciencedirect.com/science/article/pii/S0013468611017397
16 Z. Jianhui, J. Jian, L. Jinping, D. Ruimin, L. Yuanyuan, D. Hao, F. Yamin, W. Guangming, and H. Xintang : RSC Adv. **1** (2011) 1020. https://pubs.rsc.org/en/Content/ArticleLanding/2011/RA/c1ra00280e#!divAbstract
17 S. Qu, M. He, W. Huimin, Z. Xiuhua, and W. Shengfu: Sens. Actuators, B **203** (2014) 588. https://www.sciencedirect.com/science/article/pii/S0925400514007795
18 J. Chen and J. Zheng: J. Electroanal. Chem. **749** (2015) 83. https://www.sciencedirect.com/science/article/pii/S1572665715002192
19 L. Weiwei, O. Ruizhuo, Z. Wangyao, Z. Shuang, Y. Yang, J. Yajun, Y. Yang, F. Kai, L. Xiaocai, X. Mingshu, and M. Yuqing: Electrochim. Acta **188** (2016) 197. https://www.sciencedirect.com/science/article/pii/S0013468615309269
20 F. Kurniawan, V. Tsakova, and V. M. Mirsky: Electroanalysis **18** (2006) 1937. https://onlinelibrary.wiley.com/doi/abs/10.1002/elan.200603607